AUT Journal of Modeling and Simulation

AUT J. Model. Simul., 49(2)(2017)199-208
DOI: 10.22060/miscj.2017.12177.5010

Saturated Neural Adaptive Robust Output Feedback Control of Robot Manipulators: An Experimental Comparative Study

M. Pourrahim, K. Shojaei*, A. Chatraei, O. Shahnazari

Dept. of Electrical Engineering, Najafabad Branch, Islamic Azad University, Najafabad, Iran

ABSTRACT: In this study, an observer-based tracking controller is proposed and evaluated experimentally to solve the trajectory tracking problem of robotic manipulators with the torque saturation in the presence of model uncertainties and external disturbances. In comparison with the state-of-the-art observer-based controllers in the literature, this paper introduces a saturated observer-based controller based on a radial basis function neural network. This technique helps the controller produce feasible control signals for the robot actuators. As a result, it efficiently diminishes the actuators saturation risk and consequently, a better transient performance is obtained. The stability analyses of the dynamics of the tracking errors and state estimation errors are given with the help of a Lyapunov-based stability analysis method. The theoretical analyses will systematically prove that the errors are semi-globally uniformly ultimately bounded and they converge to a small set around the origin whose size is adjustable by a suitable tuning of parameters. At last, some real experiments are performed on a laboratory robotic arm to illustrate the efficiency of the proposed control system for real industrial applications.

Review History:

Received: 18 November 2016
Revised: 11 February 2017
Accepted: 27 February 2017
Available Online: 12 March 2017

Keywords:

Actuator saturation
Adaptive robust control
Observer-based control
RBF neural networks
Robot manipulators

1- Introduction

Many research efforts have been accomplished in the recent decades where the various nonlinear control methods have been utilized to address the controller design of robot manipulators with limited inputs. One interesting aspect is the design and development of output feedback controllers (OFBCs), that eliminate velocity sensors to improve the noise immunity and save the volume, cost, and weight of the robot control system [1-4]. A main deficiency in the most of available works in the literature is that they suppose robot actuators are able to receive every arbitrary amount of generated control signals. In reality, robot actuators are subjected to physical constraints which restrict the amplitude of the available torques. Some problems that may be the result of the implementation of controllers based on the unlimited available torque assumption are: (i) degraded link position tracking, and (ii) thermal and mechanical damage. To overcome this problem, some researchers have proposed saturated tracking controllers [5-11]. A controller with limited amplitude signals has been designed in [5] for robot manipulators in the presence of uncertainties in the dynamic and kinematic models. In [6], an adaptive controller with bounded signals and a guaranteed robustness performance has been proposed for the tracking control of robotic arms. Dixon et al. [7] have introduced a tracking control law for robotic arms with bounded torque inputs. Reference [8] has proposed a bounded feedback controller to solve the robot trajectory tracking problem with the saturation constraint. The saturation function such as the hyperbolic tangent one has been used to design bounded tracking controllers for robotic arms in [9-11] in which a PID controller has been employed in their schemes. Loria et al. [12] presented a global output feedback regulator with bounded signals for the first time for robotic manipulators in 1997. However, they have not addressed the control problem under model uncertainties. Later, this work was improved by the theory of singularly perturbed systems [13].

In this paper, mathematical properties of the hyperbolic tangent function, generalized saturation functions, adaptive robust techniques, and artificial neural network (ANN)-based estimation capabilities are efficiently combined to address the above problems by proposing a saturated output feedback controller (SOFBC) for the robot trajectory tracking problem for the first time.

The remaining parts of this paper are categorized in the following order. In section 2, preliminaries and basic mathematical theories are presented. A saturated output feedback tracking control system is introduced in section 3. The experimental results are provided in section 4 to demonstrate the superiority of the proposed controller. Eventually, section 5 concludes the paper.

2- Preliminaries

In this section, we briefly review some background materials required in this paper.

2- 1- Robotic Arm Model

The dynamic equation of a rigid n-link direct-drive robot is demonstrated by the following form:

$$M(q)\ddot{q} + C(q,\dot{q})\dot{q} + D\dot{q} + G(q) + \tau_d = \tau_a \qquad (1)$$

where the signals $q(t), \dot{q}(t), \ddot{q}(t) \in \mathrm{R}^n$ represent the link position, velocity and acceleration vectors, respectively; $M(q) \in R^{n\times n}$ shows the inertia matrix and $C(q,\dot{q}) \in \mathrm{R}^{n\times n}$ denotes a matrix of the centripetal and Coriolis terms. The

The corresponding author; Email: shojaei@pel.iaun.ac.ir

matrix $D \in R^{n\times n}$ is the diagonal positive-definite damping matrix. The vector $G(q) \in R^n$ points out the gravity effects; $\tau_d(t) \in R^n$ is a vector of external disturbances and static friction, and $\tau_a = [\tau_{a1}, \tau_{a2}, ..., \tau_{an}]^T \in R^n$ demonstrates a vector of input torques with $|\tau_{ai}| \le \tau_{ai}^{\max}, i = 1,2,...,n$.

The model (1) satisfies the following properties:

Property 1 [10], [14], [15]: The mass and inertia matrices satisfy the important property $M(q) = M^T(q) > 0$ such that

$$\lambda_m \|x\|^2 \le x^T \mathrm{M}(q) x \le \lambda_M \|x\|^2 \ \forall x, q \in \mathrm{R}^n \quad \text{,and } 0<\lambda_m \le \lambda_M < \infty$$

where $\lambda_M := \max_{\forall q \in \mathrm{R}^n} \lambda_{max}(M(q))$ and $\lambda_m := \min_{\forall q \in \mathrm{R}^n} \lambda_{min}(M(q))$.

The operators λ_{max} and λ_{min} yield the largest and smallest eigenvalues associated with the matrix M(q), respectively.

Property 2 [14]-[15]: The Coriolis and centripetal matrices meet the following properties:

2.1) $x^T \left(\dot{M}(q,\dot{q}) - 2C(q,\dot{q}) \right) x = 0, \ \forall x, q, \dot{q} \in \mathrm{R}^n$;

2.2) $\dot{M}(q,\dot{q}) = C(q,\dot{q}) + C^T(q,\dot{q}), \ \forall q, \dot{q} \in \mathrm{R}^n$;

2.3) $C(q,x_1)x_2 = C(q,x_2)x_1, \ \forall x_1, x_2, q \in \mathrm{R}^n$;

2.4) $C(q,x_1+x_2)y = C(q,x_1)y + C(q,x_2)y, \ \forall x_1, x_2, q, y \in \mathrm{R}^n$;

2.5) $\|C(q,x_1)x_2\| \le \lambda_c \|x_1\| \|x_2\|, \ \forall x_1, x_2, q \in \mathrm{R}^n, \ \forall \lambda_c \ge 0$;

Property 3 [14]-[15]: The vector of gravity is bounded as $\|G(q)\| \le \lambda_G, \forall q \in \mathrm{R}^n$, where λ_G is an unknown positive scalar constant.

Property 4 [14]: The matrix D satisfies $D = D^T > 0$,

$$\lambda_d \|x\|^2 \le x^T D x \le \lambda_D \|x\|^2 \ \forall x \in \mathrm{R}^n \quad \text{and } 0<\lambda_d \le \lambda_D < \infty$$

where $\lambda_d := \lambda_{min}(D)$ and $\lambda_D := \lambda_{max}(D)$.

Property 5 [6], [19]: The positive scalars ζ_M, ζ_C, ζ_D and ζ_G exist for all $q, q_d, \dot{q}_d \in \mathrm{R}^n$ such that:

$$\|M(q) - M(q_d)\| \le \zeta_M \|s(q - q_d)\|$$
$$\|C(q,\dot{q}_d) - C(q_d,\dot{q}_d)\| \le \zeta_C \|\dot{q}_d\| \|s(q - q_d)\|$$
$$\|D(q) - D(q_d)\| \le \zeta_D \|s(q - q_d)\|$$
$$\|G(q) - G(q_d)\| \le \zeta_G \|s(q - q_d)\|$$

2- 2- Control objectives

The following control objective is of interest in this paper:

Let $q_d(t) : [0,\infty] \to Rn$ be a smooth bounded desired trajectory that is created by a timing law. The control objective of this study is to develop a control law for a robotic arm to address the trajectory tracking problem under the following conditions:

1. The parameters of the robot manipulator's model are completely unknown and the robot is subjected to external disturbances;
2. The velocity signals are not measurable for the feedback;
3. The controller shall guarantee that input constraints are not violated in the sense that $\|\tau_a\| \le \sqrt{n}\tau_{aM}$ where $\tau_{aM} = max\{\tau_{ai,max}\}, i=1,2,...,n, \forall t \ge 0$. Subsequently, the actuator saturation problem is mitigated such that a poor transient response is prevented.
4. The controller gains can be adjusted freely without restricting their performance adjustment role.

Assumption 1. The links position signals are measurable in real-time.

Assumption 2. The reference trajectory $q_d(t)$ is selected such that $\underset{t\ge 0}{Sup}\|q_d(t)\| < B_{dp}$, $\underset{t\ge 0}{Sup}\|\dot{q}_d(t)\| < B_{dv}$ and $\underset{t\ge 0}{Sup}\|\ddot{q}_d(t)\| < B_{da}$

where B_{dp}, B_{dv} and B_{da} are bounded positive constants.

2- 3- Mathematical preliminaries

Definition 1. Given a positive scalar constant M_i, the function $s_i : R \to R : \zeta \to s_i(\zeta)$ is called a generalized saturation one with bound M_i, if it is non-decreasing, locally Lipschitz, and meets the following items:

1. $\xi s_i(\xi) > 0, \forall \xi \ne 0$
2. $|s_i(\xi)| \le M_i, \forall \xi \in \mathrm{R}$

Lemma 1. Let $s_i : R \to R : \zeta \to s_i(\zeta)$ be a generalized saturation function which is strictly increasing and continuously differentiable with the bound M_i. Let k_1 and k_2 be positive parameters and $s_i' : \xi \to ds_i / d\xi$. Then, the following always hold.

1. $y[s_i(x+y) - s_i(x)] > 0, \forall y \ne 0, \forall x \in \mathrm{R}$
2. $\lim_{|\xi|\to\infty} s_i'(\xi) = 0$
3. $s_i'(\xi)$ is bounded and positive, that is, there exists a parameter $s_{iM}' \in (0,\infty)$ such that $0 < s_i'(\xi) \le s_{iM}', \forall \xi \in R$;
4. $s_i^2(k_1\xi) / (2k_1 s_{iM}') \le \int_0^\xi s_i(kr)dr \le k_1 s_{iM}' \xi^2 / 2, \forall \xi \in \mathrm{R}$;
5. $\int_0^\xi s_i(kr)dr > 0, \forall \xi \ne 0$
6. $\int_0^\xi s_i(kr)dr \to \infty$ as $|\xi| \to \infty$
7. $|s_i(k_1x + k_2y) - s_i(k_2y)| \le s_{iM}' k_1 |x|$ and $|s_i(k_1x) - s_i(k_1x - k_2y)| \le s_{iM}' k_2 |y|, \ \forall x, y \in \mathrm{R}$;
8. $|s_i(k_1x)| \le s_{iM}' k_1 |x|, \forall x \in \mathrm{R}$;
9. From (8), it is clear that $|s_i(k_1x)|^2 \le s_{iM}' k_1 |x| |s_i(k_1x)| = s_{iM}' k_1 x s_i(k_1x), \forall x \in \mathrm{R}$;
10. From (4), it turns out that $s_i^2(\xi) \le s_{iM}'^2 \xi^2, \forall \xi \in \mathrm{R}$.

Proof. See the reference [8].

As it is conventional in the literature of the adaptive control [16], a projection operator is presented here to force the parameter estimates to remain within a bounded convex set $\psi_0 := \{\theta \in Rp : g(\theta) \le 0\}$, where $g(\theta)$ is a constraint function on θ which should be defined by the user based on a prior knowledge of θ [16]. The vector of parameters' estimates, i.e. $\hat{\theta} \in \mathrm{R}^p$, is provided by the following adaptive rule:

$$\dot{\hat{\theta}} = Proj_{\hat{\theta}}(\zeta) = \begin{cases} \zeta, & \text{if } \hat{\theta} \in \psi_\theta^0 \\ & \text{or } \hat{\theta} \in \delta(\psi_\theta) \text{ and } n_{\hat{\theta}}^T \zeta \le 0 \\ (I_p - \Gamma \dfrac{n_{\hat{\theta}} n_{\hat{\theta}}^T}{n_{\hat{\theta}}^T \Gamma n_{\hat{\theta}}})\zeta, & \text{otherwise} \end{cases} \quad (2)$$

where $\zeta \in R^p$,and ψ_θ^0 and $\delta(\psi_\theta)$ demonstrate the interior and the boundary of ψ_θ, respectively; $n_{\hat{\theta}} := \nabla g(\hat{\theta})$ is the outward unit normal vector at $\hat{\theta} \in \delta(\psi_\theta)$,where $\Gamma \in Rp \times p$ shows the adaptive gain matrix, that is symmetric and $\hat{\theta}(0) \in \psi_\theta$.

Lemma 2 [17]. A class of saturation functions $s_{hi}(\xi)$ with the property $|s_{hi}(\xi)| \le 1, \forall \xi \in R$ exist such that $xs_{hi}(x) \ge 0$ and $h|x| \le xhs_{hi}(vhx/\gamma_d) + \gamma_d$ hold for any $\gamma_d > 0$ and $\forall x,h \in R$ where v denotes a parameter which satisfies the equality $v = e - (v+1)$, that yields $v = 0.2785$.

2- 4- RBF neural network

In this subsection, RBFNN is presented to estimate uncertain nonlinear functions of the robot dynamics. Fig. 1 shows the structure of a three-layer RBFNN. This structure is extensively employed to approximate uncertain functions [14], [18].

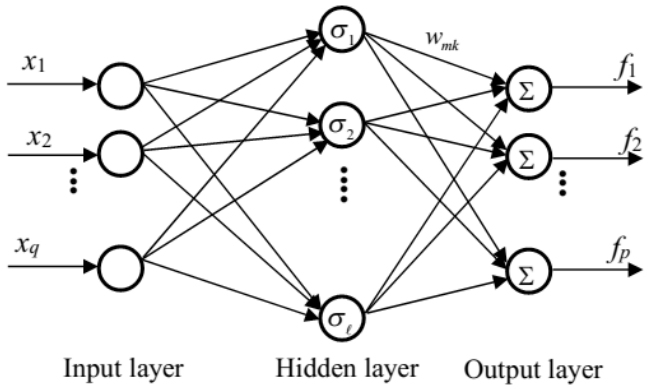

Fig. 1. A radial basis function neural network

An RBFNN for an arbitrary continuous function $f(x): U \to Rp$, where U denotes a compact set, is written in the following form:

$$f(x) = \sum_{k=1}^{\ell} w_{mk} \sigma_k(x) + \varepsilon_m \qquad m = 1,2,\ldots,p,$$
$$\sigma_k(x) = \exp\left(-\frac{x - \mu_k^2}{\lambda_k^2}\right) \qquad k = 1,2,\ldots,\ell \quad (3)$$

where ε_m is the approximation error of RBFNN, l and p are representing the number of nodes in the hidden and output layers, respectively, $\sigma_k(x)$ is k-th Gaussian basis function where $\mu_k = [\mu_{k1}, \mu_{k2}, \ldots, \mu_{kq}]^T$ shows the center vector and λ_k denotes the standard deviation. Then, the nonlinear function is stated by the following expression:

$$f(x) = W \sigma(x) + \varepsilon \quad (4)$$

where $f(x) = [f_1(x), \ldots, f_p(x)]^T$, $W \in R^{p \times l}$ shows the matrix of weights, $\sigma(x) = [\sigma_1(x), \ldots, \sigma_l(x)]^T$ and $\varepsilon = [\varepsilon_1, \varepsilon_2, \ldots, \varepsilon_p]^T$ is bounded as $||\varepsilon|| \le B_\varepsilon$ with the upper bound B_ε. Therefore, the uncertain nonlinear function is estimated as $\hat{f}(x) = \hat{W}\sigma(x)$ where $\hat{W}$ displays the estimation of the weights matrix, that should be updated by designing an adaptation rule.

3- Bounded Nn-based OFBC

3- 1- Controller development

A bounded RBFNN-based adaptive robust OFB controller is designed here to meet the conditions (i)-(iv). To systematically design the observer and controller, the tracking error is specified by $e(t) := q(t) - q_d(t)$ and the state observation error is described by $z(t) := q(t) - \hat{q}(t)$. The signal $\hat{q}(t)$ shows the estimation of $q(t)$. Then, the following signals are taken into account:

$$\dot{q}_r = \dot{q}_d - \Lambda s(q - q_d) = \dot{q}_d - \Lambda s(e) \quad (5)$$
$$r_1 = \dot{q} - \dot{q}_r = \dot{e} + \Lambda s(e) \quad (6)$$
$$\dot{q}_o = \dot{\hat{q}} - \Lambda s(z) \quad (7)$$
$$r_2 = \dot{q} - \dot{q}_o = \dot{z} + \Lambda s(z) \quad (8)$$

where $s(x) := [s_1(x_1), \ldots, s_n(x_n)]^T$, $\forall x \in R^n, s_i(\bullet)$, $i = 1,\ldots,n$ is defined by Definition 1, $\dot{q}_r, \dot{q}_o \in R^n$ are the variables of the controller and observer [19] and $\Lambda = \Lambda^T \in R^{n \times n}$ shows a diagonal positive-definite matrix. By inserting (6) in (1), and using Properties 2.3 and 2.4, the following open-loop error dynamics is achieved:

$$\begin{aligned} M(q)\dot{r}_1 = & -C(q,\dot{q})r_1 - Dr_1 + \tau_a - C(q,\dot{q}_r)\dot{e} \\ & + M(q)\Lambda s'(e)\dot{e} + C(q,\dot{q}_d)\Lambda s(e) \\ & + D\Lambda s(e) + \tilde{\xi} + \xi_d - \tau_d \end{aligned} \quad (9)$$

where

$$\begin{aligned} \tilde{\xi} = & (M(q_d) - M(q))\ddot{q}_d + (C(q_d,\dot{q}_d) - C(q,\dot{q}_d))\dot{q}_d \\ & + (D(q_d) - D(q))\dot{q}_d + G(q_d) - G(q) \end{aligned}$$

which is bounded as $\|\tilde{\xi}\| \le B_\xi \|s(e)\|$ by using Property 5, where $B_\xi = \zeta_M B_{da} + \zeta_c B_{dv}^2 + \zeta_G$.

Also, $\xi_d = -M(q_d)\ddot{q}_d - C(q_d,\dot{q}_d)\dot{q}_d - D\dot{q}_d - G(q_d)$ is the desired computed dynamics of the robot, which is stated as $\xi_d(x_d) = W\sigma(x_d) + \varepsilon(x_d)$. Then, the following saturated neural network adaptive robust OFBC controller is proposed in this paper:

$$\begin{aligned} \tau_a(t) = & -s(K_1\dot{q}_o - K_1\dot{q}_r) - \hat{W}\sigma(x_d) \\ & - \hat{\alpha} s_h(v\hat{\alpha}(\hat{r}_1 + \hat{r}_2)/\gamma_d(t)) \end{aligned} \quad (10)$$

where $K_1 = K_1^T \in R^{n \times n}$ is a matrix which is positive-definite. The parameter $\hat{\alpha}$ and ANN weights matrix are generated by

$$\dot{\hat{W}} = \text{Proj}_{\hat{W}}(\Gamma_W(\hat{r}_1 + \hat{r}_2)\sigma^T(x_d)) \quad (11)$$
$$\dot{\hat{\alpha}} = \text{Proj}_{\hat{\alpha}}(\gamma_\alpha \|\hat{r}_1 + \hat{r}_2\|) \quad (12)$$

where Γ_w and γ_a denote the adaptation gain matrices. It is necessary to mention that $\hat{r}_1 + \hat{r}_2$ is the approximation of $r_1 + r_2$ which is given as follows:

$$\hat{r}_1 + \hat{r}_2 := \dot{\hat{q}} - \dot{q}_d + \Lambda s(e) + \Lambda s(z) \quad (13)$$

The approximation $\hat{r}_1 + \hat{r}_2 \cong r_1 + r_2$ can be confirmed if the gains Λ and k_d are selected large enough where k_d is the

gain of the state estimator, which will be introduced below. For the aim of the stability analysis in the next subsection, the approximation error is defined by

$$\tilde{r}_1+\tilde{r}_2 := r_1+r_2-(\hat{r}_1+\hat{r}_2)=2(r_2-\Lambda s(z))$$

from (6), (8) and (13) which is bounded as:

$$\|\tilde{r}_1+\tilde{r}_2\|\le \xi_5\|x\| \tag{14}$$

where ξ_5 represents a positive constant. Now, a velocity estimator is proposed as follows which is inspired by the reference [19]:

$$\dot{\hat{q}}(t)=\dot{\hat{q}}_o(t)+\Lambda s(z(t))+k_d z(t) \tag{15}$$

$$\dot{\hat{q}}_o(t)=\dot{q}_d(t)+k_d\Lambda\int_0^t s(z(\tau))d\tau \tag{16}$$

where $k_d\in R$ shows the gain of the state estimator which is a positive constant. To run the observer, the initial values of the states are chosen as follows:

$$\dot{\hat{q}}_o(0)=-(\Lambda s(z(0))+k_d z(0)),\hat{q}(0)=q(0)$$
$$z(0)=0 \text{ and } \dot{\hat{q}}(0)=0$$

Then, considering that $r_1-r_2=\dot{q}_o-\dot{q}_r$ from (6) and (8) and substituting (10) in (9), the closed-loop system error dynamics is achieved as follows:

$$\begin{aligned}M(q)\dot{r}_1=&-C(q,\dot{q})r_1-Dr_1-s(K_1r_1-K_1r_2)\\&-\hat{W}\sigma(x_d)-\hat{\alpha}s_h(\upsilon\hat{\alpha}(\hat{r}_1+\hat{r}_2)/\gamma_d(t))\\&+W\sigma(x_d)+\varepsilon(x_d)+\chi_1-\tau_d\end{aligned} \tag{17}$$

where

$$\begin{aligned}\chi_1=&-C(q,\dot{q}_r)\dot{e}+C(q,\dot{q}_d)\Lambda s(e)\\&+M(q)\Lambda s'(e)\dot{e}+D\Lambda s(e)+\tilde{\xi}\end{aligned} \tag{18}$$

whose upper bound is expressed as follows by using Properties1, 2.5 and 4:

$$\|\chi_1\|\le\xi_1\|x\|+\xi_2\|x\|^2 \tag{19}$$

where $\xi_1,\xi_2\in R$ are the positive upper-bounding constants. Also, $x\in R^{4n}$ is defined as follows:

$$x:=\left[s^T(e),s^T(z),r_1^T,r_2^T\right]^T \tag{20}$$

If the weights matrix estimation error is defined by $\tilde{W}=W-\hat{W}$, one attains

$$\begin{aligned}&W\sigma(x_d)+\varepsilon(x_d)-\hat{W}\sigma(x_d)\\&=\tilde{W}\sigma(x_d)+\varepsilon(x_d)\end{aligned} \tag{21}$$

By inserting (21) in (17), the following error dynamic equation is established:

$$\begin{aligned}M(q)\dot{r}_1=&-C(q,\dot{q})r_1-Dr_1-s(K_1r_1-K_1r_2)\\&-\hat{\alpha}s_h(\upsilon\hat{\alpha}(\hat{r}_1+\hat{r}_2)/\gamma_d(t))\\&+\tilde{W}\sigma(x_d)+\varepsilon(x_d)-\tau_d+\chi_1\end{aligned} \tag{22}$$

The time derivative of (15) results in $\ddot{\hat{q}}=\ddot{\hat{q}}_o+\Lambda s'(z)\dot{z}+k_d\dot{z}$ which is equal to $\dot{r}_1=\dot{r}_2+k_d r_2+\Lambda s'(e)\dot{e}$ by applying (6) and (8). The Properties 2.3 and 2.4 help write (22) as:

$$\begin{aligned}M(q)\dot{r}_2=&-C(q,\dot{q})r_2-k_dM(q)r_2\\&-s(K_1r_1-K_1r_2)-\hat{\alpha}s_h\\&(\upsilon\hat{\alpha}(\hat{r}_1+\hat{r}_2)/\gamma_d(t))+\tilde{W}\sigma(x_d)\\&+\varepsilon(x_d)+\chi_2-\tau_d\end{aligned} \tag{23}$$

where

$$\begin{aligned}\chi_2=&-Dr+D\Lambda s(e)+C(q,r_1+\dot{q}_r)r_2\\&-C(q,r_1)(r_1+2\dot{q}_r)\\&+C(q,\Lambda s(e))(\dot{q}_r+\dot{q}_d)+\tilde{\xi}\end{aligned} \tag{24}$$

From (3) and (4), Properties 2.5 and 4, and Lemma 1, an upper bound for χ_2 is acquired as follows:

$$\|\chi_2\|\le\xi_3\|x\|+\xi_4\|x\|^2 \tag{25}$$

where $\xi_1,\xi_2\in R$ are some positive parameters.

3- 2- Analysis of closed-loop stability

The stability of the control system is analyzed here by the following theorem:

Theorem 1: Let the dynamic model of robot manipulators be given by (1). Consider a continuous bounded desired trajectory under Assumptions 1–2. If the gains of the following proposed controller:

$$\tau_a(t)=-s(K_1\dot{q}_o-K_1\dot{q}_r)-\hat{W}\sigma(x_d)-u_R$$
$$u_R=\hat{\alpha}s_h(\upsilon\hat{\alpha}(\hat{r}_1+\hat{r}_2)/\gamma_d(t))$$
$$\dot{\hat{W}}=\mathrm{Proj}_{\hat{W}}(\Gamma_W(\hat{r}_1+\hat{r}_2)\sigma^T(x_d))$$
$$\dot{\hat{\alpha}}=\mathrm{Proj}_{\hat{\alpha}}(\gamma_\alpha\|\hat{r}_1+\hat{r}_2\|)$$
$$\hat{r}_1+\hat{r}_2:=\dot{\hat{q}}-\dot{q}_d+\Lambda s(e)+\Lambda s(z)$$

satisfy the following inequalities:

$$\lambda_{\min}(\Lambda)>0.5 \tag{26}$$

$$\lambda_d>s'_{MM}k_{1M}+0.5+0.5(\xi_1+\xi_2) \tag{27}$$

$$k_d>(2s'_{MM}k_{1M}+0.5+0.5(\xi_3+\xi_4))/\lambda_m \tag{28}$$

where $k_{1M}=\lambda_{\max}(K_1)$ and $s'_{MM}:=\max\{s'_{iM}\}_{i=1}^n$, then, the proposed bounded RBF neural network adaptive robust OFBC guarantees (i) the boundedness of all closed-loop signals, and (ii) the semi-global uniform ultimate boundedness (SGUUB) of the tracking and observation errors. In addition, an estimation of the region of attraction is given by

$$R_A=\left\{\vartheta\in\Re^p\;\middle|\;\|\vartheta\|<\sqrt{\frac{2\beta_m-(\xi_1+\xi_3+\xi_5)}{(\xi_2+\xi_4)(\lambda_\vartheta/\lambda_x)}}\right\}$$

where $\vartheta:=[\upsilon^T,\tilde{w}_{11},...,\tilde{w}_{p\ell},\tilde{\alpha}]^T$, $\upsilon=\left[e^T,z^T,r_1^T,r_2^T\right]^T$ $P=4n+pl+1$, β_m is a positive parameter which depends on control gains, ξ_i, $i=1,...,5$ are defined in (14), (19) and (25), and λ_x and λ_υ will be given later.

Proof: See the appendix section

Remark 1 (guidelines for parameters tuning):
In practical situations, the accurately tuning of the controller's parameters is a little cumbersome and it is often done by the trial and error methods. In this remark, a few guidelines are given for the users to adjust the control parameters properly. The controller's parameters K_1, Λ, k_d, Γ_w, γ_a and $\gamma_d(t)$ should be tuned carefully to adjust the transient and steady-state performances. Based on Lyapunov stability analysis which is presented in the appendix section, the following laws are provided here for a trade-off between the robustness and the tracking performance of the control system:

i. Controller and observer gains: The increasing of gains of the controller and the observer, i.e. K, Λ, and k_d, increase the convergence rate c_m in (41) and consequently lead to a smaller γ_{lim}/c_m. In addition, an arbitrary increase in K_1 does not change the amplitude of the control signals in the present controller (10) by recalling the saturation function properties in Lemma 1.

ii. Artificial neural network parameters: At first, a small number of neurons in the hidden layer are selected, then, one gradually increases this to gain a better performance for the trajectory tracking. The number of neurons is enough when there is no performance improvement. Large values of ANN gain, Γ_w, in (11) increase the rate of uncertain nonlinearities learning. However, it should be noted that the stability of the system might be jeopardized by choosing very large gains and the speed of learning is decreased by the selection of very small gains.

iii. Adaptive robust control parameters: The increase of adaptive gain γ_a in the update rule (12) improves the robustness and the tracking performance of the controller. It should be noted that larger values of the adaptive gain γ_a may increase the roughness of the control signals. It in turn leads to an unwanted chattering in the control signals which is impractical for the robot motors due to their restricted bandwidth. One can make a trade-off between the smoothness of the controller signals and the final tracking accuracy by a finely tuning of the time function $\gamma_d(t)$ in the controller (10). The controller (10) generates smoother signals by setting a large value of $\gamma_d(t)$. However, it should be noted that a larger magnitude of $\gamma_d(t)$ increases the magnitude of γ_{lim} in (41). Hence, a larger ultimate bound, i.e. γ_{lim}/c_m, is resulted and, thus, the final tracking error will be increased.

4- Experimental Evaluation

4- 1- Experimental results

Here, the proposed controller is implemented on an industrial robot, SCARA IBM 7547 shown in Fig. 2. For the definition of the kinematics and dynamics of this type of robotic arms, the interested readers are referred to robotic textbooks [14-15] and references therein.

This robot is a 4-DOF IBM 7547 SCARA robot manipulator which has three rotational joints and one prismatic joint is driven by gearbox DC motors equipped with incremental shaft encoders.

The controller signals are converted to 40 KHz PWM signals with 13 bits resolution, which are directly applied to DC motors via IRF540N-MOSFET (H-Bridge technique) power amplifiers according to Fig. 3. The control system of the robot has been designed and implemented on an Arduino Due board. This board uses Atmel SAM3X8E ARM Cortex-M3 CPU microcontroller with 84 MHz clock frequency, 54 digital I/O pins (where twelve pins can be utilized for PWM outputs), 12 analog inputs and 4 UARTs (serial inputs of the hardware). The test bed consists of a 4-DOF SCARA industrial robot, decoder counter latch, MOSFET power amplifier and Arduino Due controller is connected to a computer as shown in Fig. 4. In this figure, the required hardware for the implementation of the proposed controller has been illustrated completely. The following saturation function is selected in this experiment to bound the tracking and estimation errors in order to evaluate the proposed saturated observer-based controller:

$$s_j(\eta_j)=\begin{cases}-L_j+(M_j-L_j)\tanh\left(\dfrac{\eta_j+L_j}{M_j-L_j}\right), & \forall \eta_j<-L_j\\ \eta_j, & \forall \eta_j<-L_j\\ L_j+(M_j-L_j)\tanh\left(\dfrac{\eta_j-L_j}{M_j-L_j}\right), & \forall \eta_j<-L_j\end{cases} \quad (29$$

Fig. 2. SCARA IBM 7547 robot manipulator.

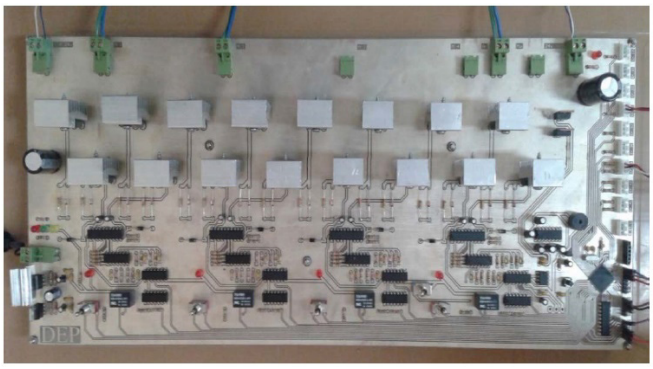

Fig. 3. MOSFET Power Amplifier

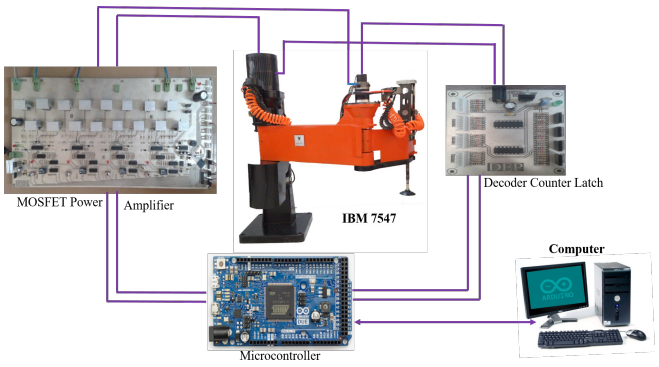

Fig. 4. The block diagram of the implementation system

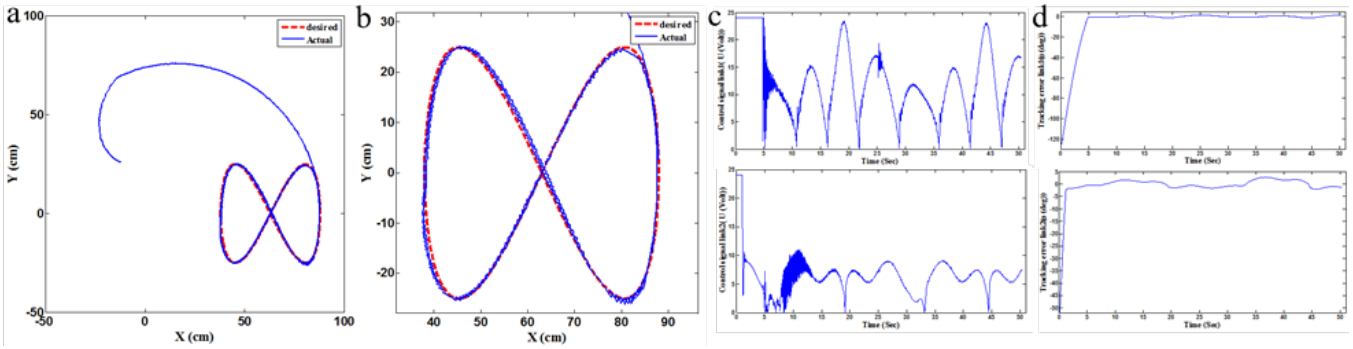

Fig. 5. Trajectory tracking results on SCARA IBM7547 robot manipulator without saturation: (a) robot and desired trajectories, (b) a magnified view of the trajectory, (c) controller output signals, and (d) the tracking errors.

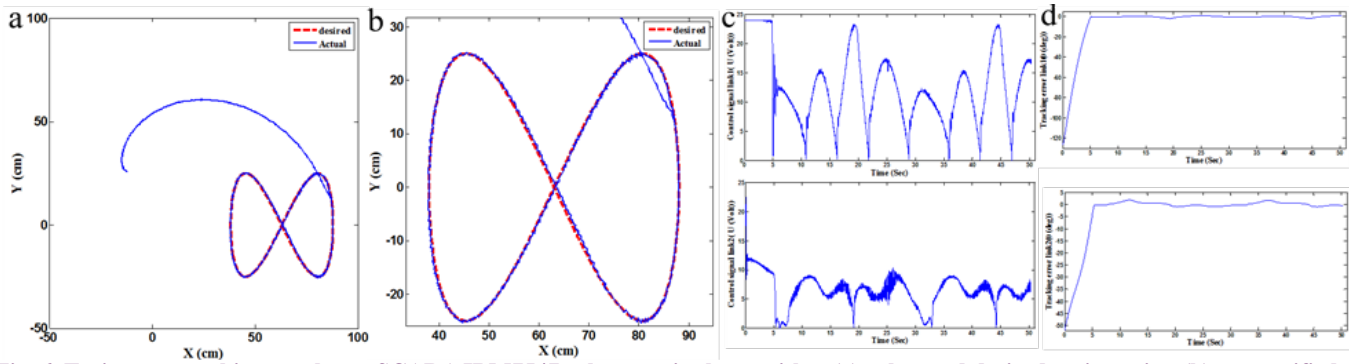

Fig. 6. Trajectory tracking results on SCARA IBM7547 robot manipulator with : (a) robot and desired trajectories, (b) a magnified part of the trajectory, (c) controller output signals and (d) the tracking errors.

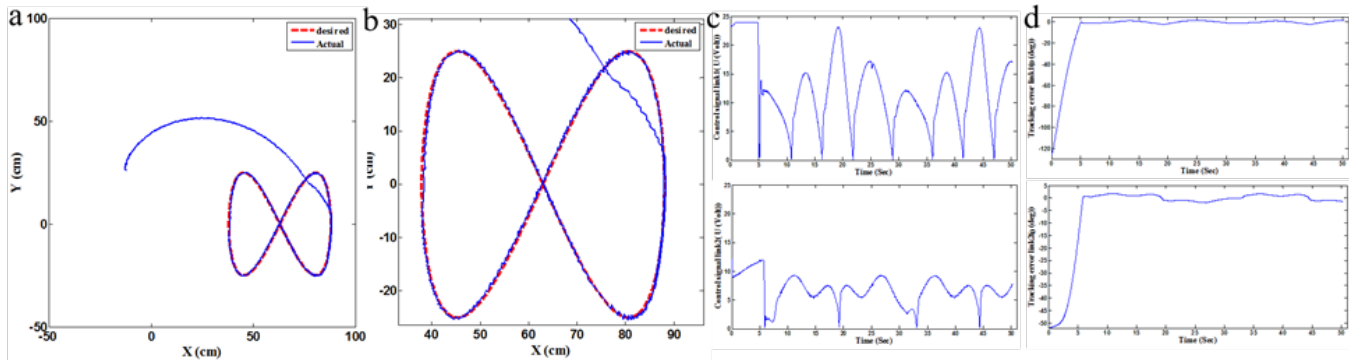

Fig. 7. Trajectory tracking results on SCARA IBM7547 robot manipulator with : (a) robot and desired trajectories, (b) a magnified view of the trajectory, (c) controller output signals and (d) the tracking errors.

Table I. Quantitative comparisons

Performance index	Proposed controller in [2]		Proposed controller with tanh(.)		Proposed controller of this paper	
	Link 1	Link 2	Link 1	Link 2	Link 1	Link 2
rms(e(t)) (m)	21.1701	10.1309	21.2460	10.3058	21.5090	11.0610
rms(u(t)) (V)	14.9235	7.2507	13.0695	6.9656	12.9680	5.2013
e_M(m)	53.0414	21.4433	53.2399	26.7734	53.8735	28.1524
e_f(m)	1.1607	1.4758	0.8866	1.0715	0.7845	0.5397

where $L_j<M_j$, $j=1,2$ denotes the saturation function parameter which is chosen by the user to obtain a desired performance. In these experiments, the parameters of the controller that produce an acceptable tracking response are given by $K_1=diag[0.32,0.15]$, $\Lambda=diag[46,42]$, $k_d=18$, $\Gamma_w=2$, $\Gamma_a=0.1$, and $\gamma_d=150$. The desired trajectory is chosen as $x=63+25sin(t)$, $y=25sin(2t)$ for this experiment. In this experiment, according to our previous paper [20], the robot is commanded to track an infinity-shaped desired trajectory whose center and radius are set to (0.63m, 0m) and 20 cm, respectively.

Figs. 5, 6 and 7 show task space trajectories of the robot, tracking errors, and controller signals for different types of saturation functions. In order to show the robot performance in this practice, a marker is placed at the end-effector of the robot

to plot the trajectory clearly. Some different desired trajectories are commanded to the robot control system which are not shown in this paper due to space limit. All of experiments have validated the effectiveness of the proposed controller.

4- 2- Comparison of experimental results

This section assesses the controller performance for two following cases: (i) with the use of the saturation function and (ii) without any saturating function.

By comparing Fig. 6 with Fig. 7 precisely, we conclude that the use of saturation function (29) instead of a hyperbolic function improves the tracking performance and the control signals remarkably. Moreover, if the saturation function (29) is not used, non-smooth control signals are produced, which lead to serious physical damages of actuators. In the final section of this paper, a quantitative comparative evaluation will be presented.

4- 3- Quantitative comparisons

To examine the controllers' behavior, some performance criteria are considered for the experiments as follows:

- $rms(\mathrm{e}_j(\mathrm{t})) = \sqrt{\frac{1}{T_f}\int_0^{T_f} \left|e_j(\mathrm{t})\right|^2 dt}, \quad j = 1, 2$ the RMS[1] of the position error that is used to assess the average tracking performance where T_f represents the final time of the experiment and e_j represents jth position error.

- $rms(u_j(\mathrm{t})) = \sqrt{\frac{1}{T_f}\int_0^{T_f} \left|u_j(\mathrm{t})\right|^2 dt}, \quad j = 1, 2$, the RMS of control signals which is provided to examine the amount of control efforts. This index is used to determine the magnitude of the power consumption of the controller.

- $e_{M,j} = \max_t \{\left|e_j(\mathrm{t})\right|\}, j = 1, 2,$ the maximum absolute value of the position error is also used to measure the transient performance of the controllers.

- $e_{f,j} = \max_{T_f - T_L \le t \le T_f} \{\left|e_j(\mathrm{t})\right|\}$, the maximum absolute value of the position error within the final T_L seconds of the experiment is utilized to evaluate the final tracking accuracy of all controllers.

Finally, Table I shows the superiority of the proposed controller in comparison with [2] with different saturation conditions.

5- Conclusion

In this paper, a neural network-based adaptive robust controller has been designed to tackle the trajectory tracking problem for robotic arms in the absence of velocity signals and in the presence of the input saturation and modeling errors. The saturation functions have been used efficiently to confine the error signals in the controller and observer laws for diminishing the actuator saturation risk. A stability analysis based on Lyapunov theory has been applied to demonstrate the semi-global stability of the state observation and tracking errors. The experimental results were given on a laboratory robotic arm to validate that the proposed controller is effective in the presence of actuators saturation and uncertainties. A comparison was made to depict the superiority of the proposed controller over the previous controllers.

1- Root Mean Square

APPENDIX

The Proof of Theorem 1. Consider the following candidate Lyapunov function,

$$\begin{aligned} E(t) = &\sum_{i=1}^{n}\int_0^{e_i} s_i(r)dr + \frac{1}{2}r_1^T M(q) r_1 \\ &+ \sum_{i=1}^{n}\int_0^{z_i} s_i(r)dr + \frac{1}{2}r_2^T M(q) r_2 \\ &+ \frac{1}{2}\mathrm{tr}\{\tilde{W}^{\mathrm{T}}\Gamma_W^{-1}\tilde{W}\} + \frac{1}{2\gamma_\alpha}\tilde{\alpha}^2 \end{aligned} \tag{30}$$

where $\tilde{W} = W - \hat{W}$ and $\tilde{\alpha} = \alpha - \hat{\alpha}$. From the item (iv) of Lemma 1, it is easy to verify that the above function is bounded as follows:

$$\begin{aligned} &\sum_{i=1}^{n} s_i^2(e_i)/(2s'_{iM}) + 0.5\lambda_m\|r_1\|^2 + \sum_{i=1}^{n} s_i^2(z_i)/(2s'_{iM}) \\ &+0.5\lambda_m\|r_2\|^2 + 0.5\lambda_{\Gamma_w}\|\tilde{W}\|_F^2 + 0.5\gamma_\alpha^{-1}|\tilde{\alpha}|^2 \le E(t) \le \\ &0.5\max\{s'_{1M},\ldots,s'_{nM}\}\|e\|^2 + 0.5\lambda_M\|r_1\|^2 \\ &+0.5\max\{s'_{1M},\ldots,s'_{nM}\}\|z\|^2 + 0.5\lambda_M\|r_2\|^2 + 0.5\lambda_{\Gamma_W}\|\tilde{W}\|_F^2 \\ &+0.5\gamma_\alpha^{-1}|\tilde{\alpha}|^2 \end{aligned} \tag{31}$$

where $\lambda_{\Gamma_w} = \lambda_{\min}(\Gamma_W^{-1})$, and $\lambda_{\Gamma_W} = \lambda_{\max}(\Gamma_W^{-1})$. Then, (31) is expressed again in the following form:

$$\begin{aligned} &\lambda_x\|x\|^2 \le \lambda_x\|x\|^2 + 0.5\lambda_{\Gamma_w}\|\tilde{W}\|_F^2 + 0.5\gamma_\alpha^{-1}|\tilde{\alpha}|^2 \\ &\le E \le \lambda_\upsilon\|\upsilon\|^2 + 0.5\lambda_{\Gamma_W}\|\tilde{W}\|_F^2 + 0.5\gamma_\alpha^{-1}|\tilde{\alpha}|^2 \le \lambda_\vartheta\|\vartheta\|^2 \end{aligned} \tag{32}$$

where $\lambda_x = \min\{\lambda_{ks,\min}, \lambda_m/2\}$

and $\lambda_\upsilon = \max\{\lambda_{ks,\max}, \lambda_M/2\}$ and

$$\begin{aligned} &\lambda_{ks,\min} := 0.5\min\{1/s'_{1M},\ldots,1/s'_{nM}\}, \\ &\lambda_{ks,\max} := 0.5\max\{s'_{1M},\ldots,s'_{nM}\}, \\ &\vartheta := [\upsilon^T, \tilde{w}_{11},\ldots,\tilde{w}_{p\ell}, \tilde{\alpha}]^T, \\ &\upsilon := [e^T, z^T, r_1^T, r_2^T]^T, \\ &\lambda_\vartheta := \max\{\lambda_\upsilon, 0.5\lambda_{\Gamma_W}, 0.5\gamma_\alpha^{-1}\} \end{aligned} \tag{33}$$

According to (32) and items (v) and (vi) in Lemma 1, one can see that *E(t)* is a descending function, positive-definite and radially unbounded. Now, the time derivative of (30) along (6), (8), (22), and (23), using Property 2.1 and considering that the facts that $\dot{\tilde{W}} = -\dot{\hat{W}}$ and $\dot{\tilde{\alpha}} = -\dot{\hat{\alpha}}$, we have:

$$\begin{aligned}\dot{E}(t) &= s^T(e)\dot{e} + r_1^T M\dot{r}_1 + 0.5r_1^T\dot{M}r_1 + s^T(z)\dot{z} \\ &\quad + r_2^T M\dot{r}_2 + 0.5r_2^T\dot{M}r_2 - \mathrm{tr}\left\{\tilde{W}^T\Gamma_W^{-1}\dot{\hat{W}}\right\} - \tilde{\alpha}\dot{\hat{\alpha}}/\gamma_\alpha \\ &= -s^T(e)\Lambda s(e) - r_1^T Dr_1 - s^T(z)\Lambda s(z) \\ &\quad - k_d r_2^T M(q)r_2 + s^T(e)r_1 - r_1^T s(K_1r_1 - K_1r_2) \\ &\quad - r_1^T\hat{\alpha}s_h(\upsilon\hat{\alpha}(\hat{r}_1+\hat{r}_2)/\gamma_d(t)) + r_1^T\tilde{W}\sigma(x_d) \\ &\quad + r_1^T\varepsilon(x_d) - r_1^T\tau_d + r_1^T\chi_1 + s^T(z)r_2 \\ &\quad - r_2^T s(K_1r_1 - K_1r_2) - r_2^T\hat{\alpha}s_h(\upsilon\hat{\alpha}(\hat{r}_1+\hat{r}_2)/\gamma_d) \\ &\quad + r_2^T\tilde{W}\sigma(x_d) + r_2^T\varepsilon(x_d) - r_2^T\tau_d + r_2^T\chi_2 \\ &\quad - \mathrm{tr}\left\{\tilde{W}^T\Gamma_W^{-1}\dot{\hat{W}}\right\} - \tilde{\alpha}\dot{\hat{\alpha}}/\gamma_\alpha\end{aligned} \tag{34}$$

A bound for the term $\varepsilon-\tau_d(t)$ is given as follows:

$$\|\varepsilon - \tau_d\| \le \alpha$$

By considering the inequality in (14), recalling $r_1 + r_2 = (\hat{r}_1 + \hat{r}_2) + (\tilde{r}_1 + \tilde{r}_2)$, adding and subtracting $\|\hat{r}_1 + \hat{r}_2\|\hat{\alpha}$, and substituting (11), (12), inequality (34) is written as follows:

$$\begin{aligned}\dot{E} &\le -\lambda_{\min}(\Lambda)\|s(e)\|^2 - \lambda_d\|r_1\|^2 - \lambda_{\min}(\Lambda)\|s(z)\|^2 \\ &\quad - k_d\lambda_m\|r_2\|^2 + r_1^T(s(K_1r_1) - s(K_1r_1 - K_1r_2)) \\ &\quad - r_1^T s(K_1r_1) + r_2^T(s(K_1r_1) - s(K_1r_1 - K_1r_2)) \\ &\quad - r_2^T s(K_1r_1) + \|s(e)\|\|r_1\| + \|r_1\|\|\chi_1\| + \|s(z)\|\|r_2\| \\ &\quad + \|r_2\|\|\chi_2\| - (\hat{r}_1+\hat{r}_2)^T\hat{\alpha}s_h(\upsilon\hat{\alpha}(\hat{r}_1+\hat{r}_2)/\gamma_d(t)) \\ &\quad - (\tilde{r}_1+\tilde{r}_2)^T\hat{\alpha}s_h(\upsilon\hat{\alpha}(\hat{r}_1+\hat{r}_2)/\gamma_d(t)) \\ &\quad + (\hat{r}_1+\hat{r}_2)^T\tilde{W}\sigma + \|\hat{r}_1+\hat{r}_2\|\hat{\alpha} + (\tilde{r}_1+\tilde{r}_2)^T\tilde{W}\sigma \\ &\quad + \|\tilde{r}_1+\tilde{r}_2\|\alpha - \mathrm{tr}\left\{\tilde{W}^T\Gamma_W^{-1}\mathrm{Proj}_{\hat{W}}(\Gamma_W(\hat{r}_1+\hat{r}_2)\sigma^T(x_d))\right\} \\ &\quad + \tilde{\alpha}\|\hat{r}_1+\hat{r}_2\| - \tilde{\alpha}\mathrm{Proj}_{\hat{\alpha}}(\gamma_\alpha\|\hat{r}_1+\hat{r}_2\|)/\gamma_\alpha\end{aligned} \tag{35}$$

By considering Lemma 2, taking the following facts into account from [16-17]:

$$(\hat{r}_1+\hat{r}_2)^T\tilde{W}\sigma - \mathrm{tr}\left\{\tilde{W}^T\Gamma_W^{-1}\mathrm{Proj}_{\hat{W}}(\Gamma_W(\hat{r}_1+\hat{r}_2)\sigma^T)\right\} \le 0,$$

$$\tilde{\alpha}\|\hat{r}_1+\hat{r}_2\| - \tilde{\alpha}\mathrm{Proj}_{\hat{\alpha}}(\gamma_\alpha\|\hat{r}_1+\hat{r}_2\|)/\gamma_\alpha \le 0,$$

$$\|\hat{r}_1+\hat{r}_2\|\hat{\alpha} - (\hat{r}_1+\hat{r}_2)^T\hat{\alpha}s_h(\upsilon\hat{\alpha}(\hat{r}_1+\hat{r}_2)/\gamma_d(t)) \le n\gamma_d,$$

and considering (19) and (25) and recalling items (vii) and (viii) in Lemma 1, we obtain:

$$\begin{aligned}\dot{E}(t) &\le -\lambda_{\min}(\Lambda)\|s(e)\|^2 - \lambda_d\|r_1\|^2 - \lambda_{\min}(\Lambda)\|s(z)\|^2 \\ &\quad - k_d\lambda_m\|r_2\|^2 - r_1^T s(K_1r_1) + s'_{MM}k_{1M}\|r_1\|\|r_2\| \\ &\quad + s'_{MM}k_{1M}\|r_2\|^2 + s'_{MM}k_{1M}\|r_2\|\|r_1\| + \|s(e)\|\|r_1\| \\ &\quad + \|s(z)\|\|r_2\| + \xi_1\|r_1\|\|x\| + \xi_2\|r_1\|\|x\|^2 \\ &\quad + \xi_3\|r_2\|\|x\| + \xi_4\|r_2\|\|x\|^2 + \|\tilde{r}_1+\tilde{r}_2\|\theta + n\gamma_d\end{aligned} \tag{36}$$

where we note that $s'_{MM} := \max\{s'_{iM}\}_{i=1}^n$ and $\theta := \|\hat{\alpha}s_h(\upsilon\hat{\alpha}(\hat{r}_1+\hat{r}_2)/\gamma_d(t))\| + \|\tilde{W}\sigma\| + \|\alpha\|$.

By considering (11) and (12) and Assumption 2, θ can be bounded as $||\theta|| \le \theta_m$. Then, by considering $2ab \le a^2+b^2$ and recalling (14), one can re-write (36) as follows:

$$\begin{aligned}\dot{E}(t) &\le -r_1^T s(K_1r_1) - \beta_1\|s(e)\|^2 - \beta_2\|s(z)\|^2 - \beta_3\|r_1\|^2 \\ &\quad - \beta_4\|r_2\|^2 + 0.5(\xi_1+\xi_3+\xi_5)\|x\|^2 \\ &\quad + 0.5(\xi_2+\xi_4)\|x\|^4 + \gamma(t)\end{aligned} \tag{37}$$

where $\gamma(t) = n\gamma_d(t) + 0.5\xi_5\theta_m^2$ and $\beta_i, i = 1,\ldots,4$ are defined as:

$$\begin{aligned}\beta_1 &= \beta_2 = \lambda_{\min}(\Lambda) - 0.5 \\ \beta_3 &= \lambda_d - (s'_{MM}k_{1M} + 0.5 + 0.5(\xi_1+\xi_2)) \\ \beta_4 &= k_d\lambda_m - (2s'_{MM}k_{1M} + 0.5 + 0.5(\xi_3+\xi_4))\end{aligned} \tag{38}$$

The control parameters are set such that $b_i>0$, $i=1,\ldots,4$. As a result, the conditions of Theorem 1 are met. Thus, (37) may be expressed as follows:

$$\begin{aligned}\dot{E}(t) &\le -(\beta_m - 0.5(\xi_1+\xi_3+\xi_5) \\ &\quad - 0.5(\xi_2+\xi_4)\|x\|^2)\|x\|^2 + \gamma(t)\end{aligned} \tag{39}$$

where $x \in R^{4n}$ is given by (20) and β_m: $min\{\beta_1,\beta_2,\beta_3,\beta_4\}$. Hence, if β_m is selected such that:

$$\beta_m > 0.5(\xi_1+\xi_3+\xi_5) + 0.5(\xi_2+\xi_4)\|x\|^2 \tag{40}$$

Then, inequality (39) can be written as

$$\dot{E}(t) \le -c_m\|x\|^2 + \gamma_{\lim} \tag{41}$$

where c_m is also a positive scalar and $\gamma_{\lim} := \lim_{t\to\infty}\gamma(t)$. This points out that $\dot{E}(t)$ is strictly negative when x(t) is out of the compact set $S_x = \left\{x(t)\middle|0 \le \|x(t)\| \le \sqrt{\gamma_{\lim}/c_m}\right\}$, which shows $E(t)$ is decreasing out of the set S_x. This gives the following result:

$$E(t) \le E(0) \le \lambda_\vartheta\|\vartheta(0)\|^2, \forall t \ge 0 \tag{42}$$

where we used inequality (32). By recalling (32) and (42), one has

$$\|x\|^2 \le \lambda_\vartheta/\lambda_x\|\vartheta(0)\|^2 \tag{43}$$

Thus, the following condition is sufficient to satisfy (40):

$$\begin{aligned}\beta_m &> 0.5(\xi_1+\xi_3+\xi_5) + 0.5(\xi_2+\xi_4)\times \\ &\quad \left(\lambda_\vartheta/\lambda_x\|\vartheta(0)\|^2\right)\end{aligned} \tag{44}$$

The above equation hints that R_A in Theorem 1 is an estimation of the attraction region whose size depends on the controller gains. As a consequence, $||x(t)||$ is SGUUB. Therefore, this result helps us to find that $e(t), z(t), r_1(t), r_2(t), \hat{W}(t), \hat{\alpha}(t) \in L_\infty$ by recalling the properties of saturation functions which are presented in Lemma 1. The above-mentioned argument is the evidence of SGUUB stability of the state estimation and tracking errors, weights, and parameters estimation errors. Furthermore, it is concluded that $\dot{e}(t), \dot{z}(t) \in L_\infty$ by considering (6) and (8). At last, equations (6) and (8), the controller (10), and Assumption 2 show that $q(t), \hat{q}(t), \dot{q}(t), \dot{\hat{q}}(t), \dot{q}_r(t), \dot{q}_o(t), \tau_a(t) \in L_\infty$. It is clear that this statement completes the proof of Theorem 1. □

REFERENCES

[1] H. Berghuis, H. Nijmeijer, A passivity approach to

controller-observer design for robots, IEEE Transactions on robotics and automation, 9(6) (1993) 740-754.

[2] M.A. Arteaga, R. Kelly, Robot control without velocity measurements: New theory and experimental results, IEEE Transactions on Robotics and Automation, 20(2) (2004) 297-308.

[3] D.J. López-Araujo, A. Zavala-Río, V. Santibáñez, F. Reyes, Output-feedback adaptive control for the global regulation of robot manipulators with bounded inputs, International Journal of Control, Automation and Systems, 11(1) (2013) 105-115.

[4] M. Mendoza, A. Zavala-Río, V. Santibáñez, F. Reyes, Output-feedback proportional–integral–derivative-type control with simple tuning for the global regulation of robot manipulators with input constraints, IET Control Theory & Applications, 9(14) (2015) 2097-2106.

[5] W.E. Dixon, Adaptive regulation of amplitude limited robot manipulators with uncertain kinematics and dynamics, IEEE Transactions on Automatic Control, 52(3) (2007) 488-493.

[6] C. Huang, X. Peng, C. Jia, J. Huang, Guaranteed robustness/performance adaptive control with limited torque for robot manipulators, Mechatronics, 18(10) (2008) 641-652.

[7] W.E. Dixon, M.S. de Queiroz, F. Zhang, D.M. Dawson, Tracking control of robot manipulators with bounded torque inputs, Robotica, 17(2) (1999) 121-129.

[8] E. Aguiñaga-Ruiz, A. Zavala-Río, V. Santibanez, F. Reyes, Global trajectory tracking through static feedback for robot manipulators with bounded inputs, IEEE Transactions on Control Systems Technology, 17(4) (2009) 934-944.

[9] A. Laib, Adaptive output regulation of robot manipulators under actuator constraints, IEEE Transactions on Robotics and Automation, 16(1) (2000) 29-35.

[10] Y. Su, P.C. Muller, C. Zheng, Global asymptotic saturated PID control for robot manipulators, IEEE Transactions on Control Systems Technology, 18(6) (2010) 1280-1288.

[11] V. Santibañez, K. Camarillo, J. Moreno-Valenzuela, R. Campa, A practical PID regulator with bounded torques for robot manipulators, International Journal of Control, Automation and Systems, 8(3) (2010) 544-555.

[12] A. Loria, R. Kelly, R. Ortega, V. Santibanez, On global output feedback regulation of Euler-Lagrange systems with bounded inputs, IEEE Transactions on Automatic Control, 42(8) (1997) 1138-1143.

[13] J. Moreno-Valenzuela, V. Santibáñez, R. Campa, On output feedback tracking control of robot manipulators with bounded torque input, International Journal of Control, Automation, and Systems, 6(1) (2008) 76-85.

[14] F.L. Lewis, D.M. Dawson, C.T. Abdallah, Robot manipulator control: theory and practice, CRC Press, 2003.

[15] M.W. Spong, S. Hutchinson, M. Vidyasagar, Robot modeling and control, Wiley New York, 2006.

[16] P.A. Ioannou, J. Sun, Robust adaptive control, PTR Prentice-Hall Upper Saddle River, NJ, 1996.

[17] B. Yao, Adaptive robust control of nonlinear systems with application to control of mechanical systems, University of California, Berkeley, 1996.

[18] L. Xu, B. Yao, Output feedback adaptive robust precision motion control of linear motors, Automatica, 37(7) (2001) 1029-1039.

[19] K. Shojaei, A. Chatraei, A Saturating Extension of an Output Feedback Controller for Internally Damped Euler-Lagrange Systems, Asian Journal of Control, 17(6) (2015) 2175-2187.

[20] M. Pourrahim, K. Shojaei, A. Chatraei, O.S. Nazari, Experimental evaluation of a saturated output feedback controller using RBF neural networks for SCARA robot IBM 7547, in: Electrical Engineering (ICEE), 2016 24th Iranian Conference on, IEEE, 2016, pp. 1347-1352.

Please cite this article using:

M. Pourrahim, K. Shojaei, A. Chatraei, O. Shahnazari, Saturated Neural Adaptive Robust Output Feedback Control of Robot Manipulators: An Experimental Comparative Study, *AUT J. Model. Simul., 49(2)(2017)199-208*.

DOI: 10.22060/miscj.2017.12177.5010